Snow Analyses

Matthias Drusch

ECMWF, Shinfield Park, Reading
RG2 9AX, United Kingdom
dar@ecmwf.int

ABSTRACT

Four different snow water equivalent data sets have been compared: (1) The high resolution Snow Data Assimilation System (SNODAS) developed at the National Operational Hydrologic Remote Sensing Center (NOHRSC), (2) the operational analysis from the European Centre for Medium-range Weather Forecasts (ECMWF) in its old version, (3) ECMWF's revised version, which became operational in 2004, and (4) Advanced Microwave Scanning Radiometer (AMSR) derived snow water equivalent. The revised ECMWF analysis agrees better than the old one with the NOHRSC product when snow extent is compared. Both global ECMWF analyses underestimate snow water equivalent in the Western US. A direct comparison betweeen analysed snow water equivalent and AMSR-E derived SWE is difficult since the satellite observations are insensitive to low and high amounts of SWE. Consequently, a validation of snow analyses based on this independent data set is not possible for large parts of the world. In general, The AMSR-E product results in lower mean snow water equivalent and snow extent than the global analyses, when only grid boxes characterized by snow water equivalent ranging from 10 mm to 250 mm are compared.

1 Introduction

About 98 % of the global seasonal snow cover is located in the Northern Hemisphere ([3]) with a mean maximum extent of nearly 50% of the land surface area ([18]). In large areas snow melt is a significant contribution to the surface water supply and the main cause of flooding. Variability in snow cover causes dramatic changes in surface albedo and consequently in the land surface energy budget. Therefore, global snow depth and snow extent are crucial parameters for the performance of numerical prediction models and for climate monitoring including re-analysis projects.
Currently, estimates of snow extent, snow depth, and snow water equivalent (SWE) are based on: (1) in-situ observations, (2) satellite observations (e.g. from the Advanced Very High Resolution Radiometer [AVHRR], Moderate-Resolution Imaging Spectroradiometer [MODIS], Special Sensor Microwave / Imager [SSM/I], Advanced Microwave Scanning Radiometer [AMSR]), or (3) numerical models. In-situ measurements have been used to calibrate and / or validate model output or satellite retrieval algorithms. Very little work has been done on the combination of all three data sources through data assimilation systems. To the author's knowledge, only the European Centre for Medium-Range Weather Forecasts (ECMWF) and the National Operational Hydrologic Remote Sensing Center (NOHRSC) combine all three data sources in their operational snow analyses. The NOHRSC analysis is performed by an analyst who defines the areas to be updated with observations through a nudging technique. This analysis is produced on a daily basis for the US domain ([5]). At ECMWF, in-situ observations and the operational NOAA NESDIS[1] snow extent data set are used together with the model forecast to analyse snow water equivalent through a Cressman Interpolation scheme ([11]). The analysis is performed globally every 6 hours. Since the NOHRSC analysis uses a sophisticated multi-layer snow model at a high resolution together with a large and diverse number of observations it is considered to be the best data set available for the US. In this study, two versions of the operational ECMWF analysis are compared against the NOHRSC analysis: 1. The operational analysis version for CY28R2 (and older cycles), which uses a snow

[1] National Oceanic and Atmospheric Administration National Environmental Satellite, Data, and Information Service

climatology and no satellite data, and 2. the revised analysis, which became operational in CY28R3 (spring 2004). In addition, SWE derived from AMSR-E is compared with the ECMWF analyses on the global scale.

2 Data sets

As already mentioned above, four different SWE data sets are compared for the US domain and the globe. In this section the individual data sets are briefly introduced. The study period comprises the period November 2003 to May 2004.

2.1 AMSR-E derived SWE at the National Snow and Ice Data Center (NSIDC)

Daily maps of global snow water equivalent have been derived from AMSR-E obsverations at the NSIDC. L2a global swath spatially resampled brightness temperatures at 18 and 37 GHz vertical polarization (T_{18v}, T_{37v}) form the data basis for the algorithm ([7]). The retrieval algorithm can be summarized in four steps:

1. Ancillary data (i.e. fractional forest (ff) cover from [19], probability of snow from [10], a land/sea/ice mask) and brightness temperatures are mapped into 25 km resolution hemispheric Ease-Grids.
2. Estimation of surface temperature following [17] and detection of snow based on threshold analysis.
3. Calculation of SWE:

$$SWE = 4.8 \times (T_{18v} - T_{36v})/(1.0 - 0.2 \times ff) \quad (1)$$

4. Temporal and spatial sampling; consistency checks.

For more details on the SWE product the reader is referred to [7].

2.2 NOHRSC SNODAS data set

The core of the SNODAS system is a spatially distributed but horizontally uncoupled energy and mass balance model with three snow layers and two soil layers. The formulations of the thermal and water balances are based on [15]. It is run daily with a spatial resolution of 1 km and hourly time step for the US domain ([6]). The model forcings comprise output from the mesoscale Rapid Update Cycle (RUC2) atmopsheric model, which is downscaled to 1 km resolution, and remotely sensed data, i.e. NESDIS GOES [2] solar radiation, NCEP Stage IV Radar precipitation analyses, and NOAA GOES / AVHRR [3] cloud cover and albedo ([5]).
Analysts decide whether remote sensing data (NOHRSC Airborne Gamma SWE and NOHRSC GOES/AVHRR) and / or ground based observations (NWS / Cooperative Observer SWE and snow depth, CADWR & BC HYDRO SWE, and NRSC SNOTEL SWE) are used to update the model through a nudging scheme. In a first step, differences between the modelled 24 hour forecast and the in-situ measurements are computed at the observation points. These differences are analysed manually to identify regions to update; satellite data are used to determine the snow edge. In the following step, differences are spatially interpolated to the model grid. From these difference fields mean hourly nudging increments are computed for the previous 6 hours. In the last step, the model is re-run for the previous six hours and the state variables are updated hourly with the 'nudging fields'. A comprehensive description of SNODAS can be found in [4], [5], and [6]. For the comparison with the ECMWF analyses the SNODAS SWE has been aggregated linearily to the reduced Gaussian grid corresponding to T511 spectral resolution.

[2] Geostationary Operational Environmental Satellites
[3] Advanced Very High Resolution Radiometer

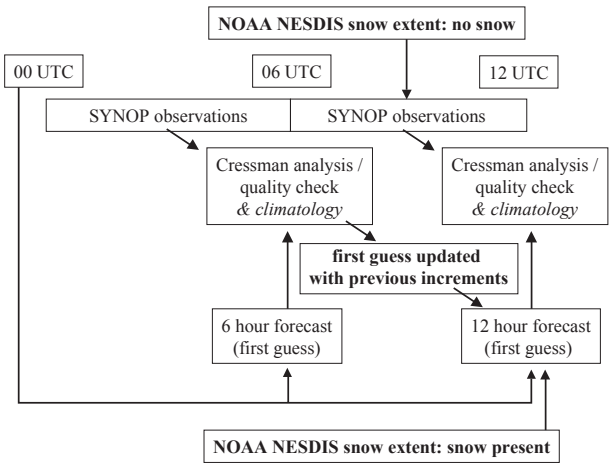

*Figure 1: Schematic view of the implementation of the operational snow analyses at ECMWF. The components shown in 'italic' are used in the OA only, the components shown in '***bold***' are used in the ROA only.*

2.3 ECMWF operational snow analyses

The current ECMWF snow depth analysis is operational since 1987, with modifications in 2001 and 2004. The snow depth analysis S^a is performed using a Cressman spatial interpolation (e.g. [9]):

$$S^a = S^b + \frac{\sum_{n=1}^{N} (S_n^o - S^{b'})}{\sum_{n=1}^{N} w_n} \tag{2}$$

where S^o are the snow depth observations from N SYNOP reports, S^b is the first guess (i.e. the 6 or 12 hour forecast), and $S^{b'}$ is the first guess field at the observation point. The weighting function w_n is defined through (1) the horizontal distance between observation and grid point and (2) a weighting function depending on the vertical displacement (i.e. the model grid point height minus observation height). For a detailed description of the analysis including the quality checks the reader is referred to [11].

In this study, two versions of the snow analysis are evaluated: (1) the operational analysis (OA), which was based on the model forecast, in-situ observations, and snow climatology ([12]) (operational from 2001 until 2004, model version CY28R2) and (2) its revised version (ROA), which became operational with model version CY28R3. In the ROA, satellite derived NOAA NESDIS snow extent is used in addition to the conventional ground based observations and the model forecast. Areas, for which the model first guess is snow free and the NOAA NESDIS product contains snow, are updated with a snow depth of 100 mm ([1]). Snow free grid boxes in the NOAA NESDIS product enter the analysis as observations with 0 mm snow depth. The relaxation to climatology is omitted in the ROA since it is expected that the satellite data can replace the role of snow depth climatological data in correcting for the model bias [11].

In addition to these changes to the analysis scheme itself, the operational implementation has been modified for the RAO compared to the OA. Both snow analyses are performed every six hours before the 12 hourly 4DVar analysis for the atmosphere starts. In the delayed cut off forecast mode ([14]) the 4 DVar 12 hour window covers 03 (15) UTC to 15 (03) UTC. As a consequence, the snow analyses are based on the 6 hour and 12 hour forecasts from 00 UTC and 12 UTC forecast base times and the observations collected in the 6 hour time period around the analysis time. In the OA, since the introduction of the 12 hour atmospheric data assimilation window, the analysis increments at 06 UTC and 18 UTC were not cycled. This was corrected in the ROA: The first guess for 00 UTC and 12 UTC (i.e. the 12 hourly forecasts) are updated with the analysis increments from the previous analyses at 6 UTC or 18 UTC. A schematic view of the implementation is given in Fig. 1.

3 Intercomparisons for the 2003 / 2004 snow season

For the intercomparison beween the different data sets, the 1 km NOHRSC analysis has been averaged linearily to the reduced Gaussian grid corresponding to T511 spatial resolution. In case of the AMSR-E 25 km product, the nearest neighbour sampling technique has been applied. Every comparison shown in the following sections has been made at T511 spectral resolution ($\approx$ 39 km).

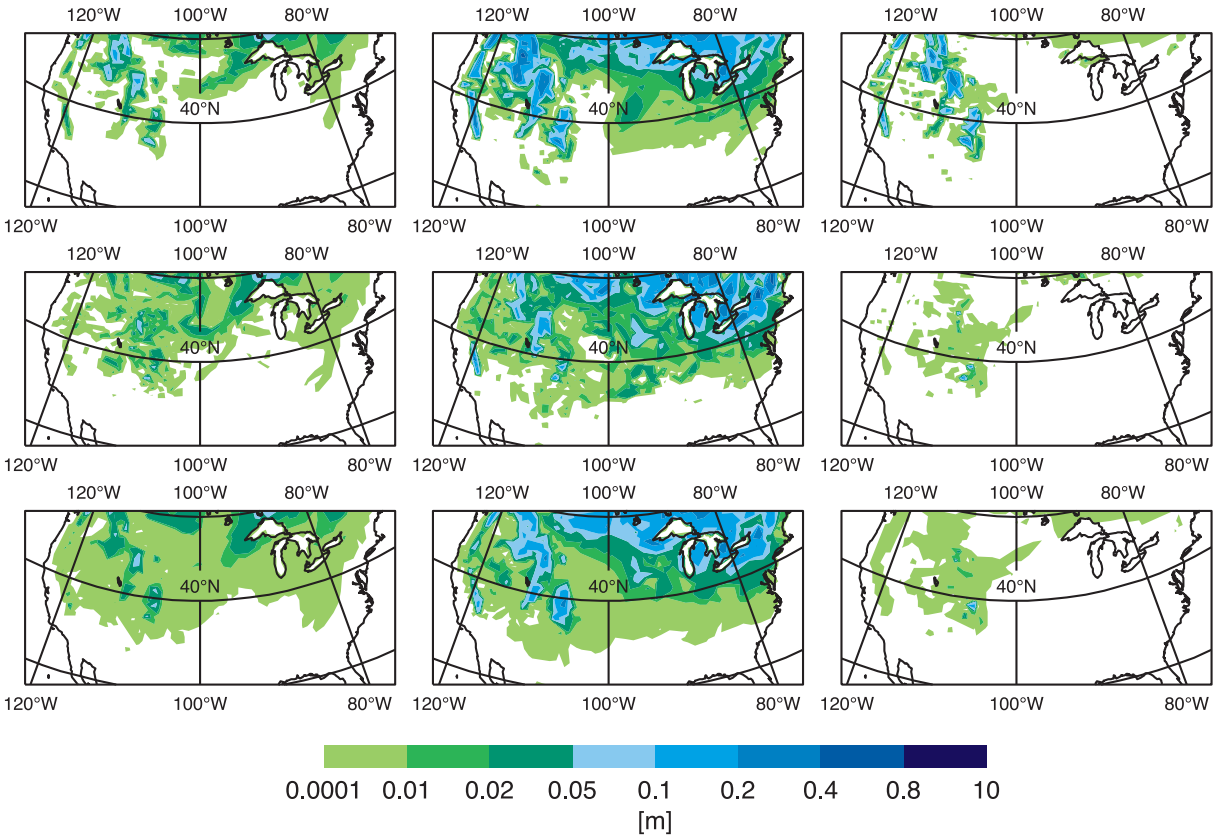

Figure 2: Analysed snow water equivalent at 06 UTC for November 30, 2003 (left column), January 31, 2004 (middle column), and April 30, 2004 (right column). The aggregated SNODAS values are shown in the top row; ROA and OA analyses are displayed in the middle and bottom row, respectively.

3.1 The conterminous US

Analysed snow water equivalent at 06 UTC for three days from the snow season 2003 / 2004 (November 30, January 31, and April 30) is given in Fig. 2. The top row shows aggregated SNODAS data sets, the middle and bottom pannels correspond to the ROA and OA, respectively. In general, the OA images, which contain the relaxation to climatology, look much smoother when compared to the other data sets. A number of small scale features, e.g. snow extent in the East in the November image, are well captured in the ROA but not in the OA. Compared to the SNODAS data set, the absolute amount of SWE seems to be smaller in both ECMWF analyses. These differences seem to be largest in the Western US. Another interesting feature to notice is the snow edge in the Central US in the January 31 image. In the revised analysis, the snow field has been updated with the NOAA NESDIS snow extent using a snow depth of 100 mm [1]. Significantly smaller values were obtained for the SNODAS product (Fig. 2, top) and through the use of climatology (Fig. 2, bottom).
A detailed comparison of the temporal evolution of mean snow extent and mean snow water equivalent is

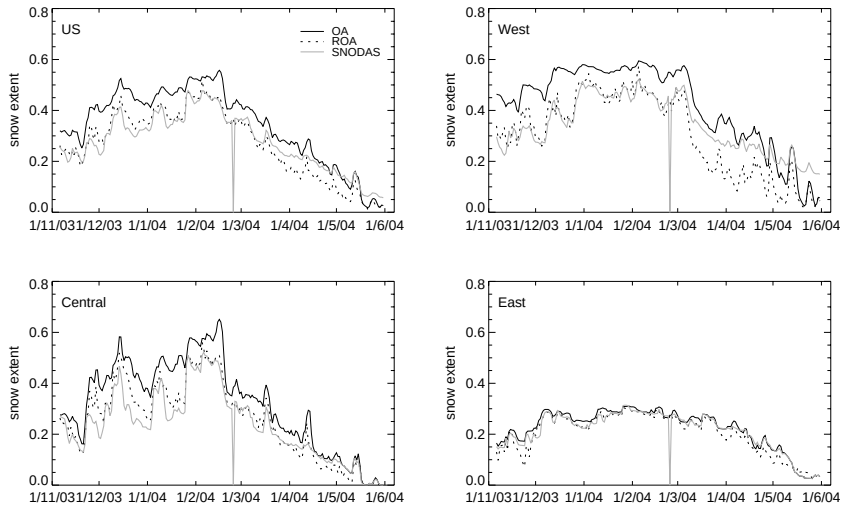

Figure 3: Mean daily snow extent for the US (upper left), the Western US (upper right), the Central US (lower left), and the Eastern US (lower right).

given in Figs. 3 and 4, respectively. For this comparison, the US domain has been divided into the West (-124° to -105° W), the Central part (-105° to -80° W), and the East (-80° to -60° W). Since fractional snow coverage is not being analysed at ECMWF, snow extent is defined through grid boxes containing snow (Fig. 3). For the Eastern part of the US the differences between the three analyses are generally small. The most significant differences can be found in the Western part. During the snow accumulation season the ROA derived snow extent is in very good agreement with the SNODAS data set. In contrast, the OA overestimates snow extent by ≈ 10 %. From the beginning of March until the beginning of April the snow extent decreases by ≈ 30 % in the ROA, compared to ≈ 20 % in the SNODAS data set. From April onwards, the difference between the ROA and the SNODAS product varies from 5 % to 10 %, the shape and slope of both curves is comparable. In contrast, the OA is in reasonable agreement with the SNODAS data set for the second half of March and the first half of April. The melting rate in the following period is higher in the OA then in the SNODAS analysis. The comparison for the Central part of the US gives similar results as for the Western part of the US. However, the differences between the analyses are smaller in these regions.

Mean daily snow water equivalent is shown in Fig. 4. Again, the differences between the three analyses for the Eastern part of the US are relatively small. In the Central US, both ECMWF analyses result in higher mean SWE values than the SNODAS product until the beginning of April. During the melting season, the OA is in very good agreement with the SNODAS product. However, given the fact that the snow extent is too high in the OA during this period, it can be assumed that the actual SWE values are too low and that the good agreement is the result of two compensating errors. The ROA is consistently too high during the melting season. It is likely that this overestimation is introduced through satellite observations, for which a constant snow depth of 100 mm has been assigned (Fig. 2). In the West, The SNODAS analysis yields significantly higher SWE values throughout the snow season. As already discussed in the previous paragraph (Fig. 2), the mountain areas seem to have too little snow in both ECMWF analyses. Apart from the systematic difference, the slope of the three curves suggest that the snow accumulation season is better captured by the OA whereas the melting season is better represented by the ROA. At this stage, it is not clear whether the differences between OA and ROA are introduced through climatology or the satellite data. It can be summarized that the differences between the analyses on the continental scale are ≈ 5 mm in SWE and 5 % in snow extent. However these values may be higher on the regional scale and certain periods of the snow season.

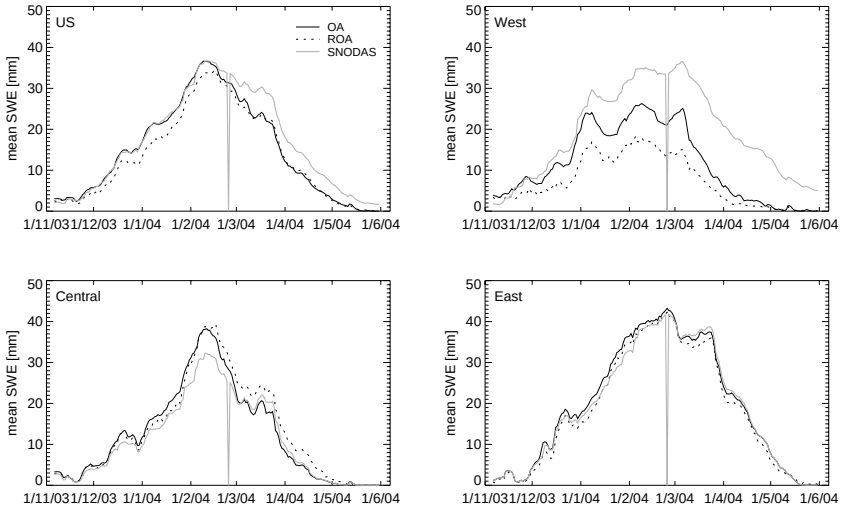

Figure 4: Mean daily snow water equivalent for the US (upper left), the Western US (upper right), the Central US (lower left), and the Eastern US (lower right).

3.2 Global comparison with AMSR-E

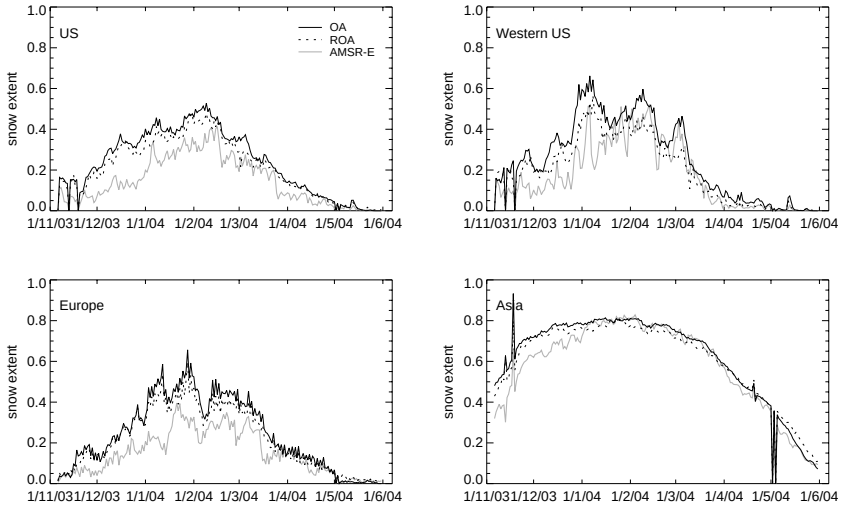

Figure 5: Mean daily snow extent for the US (upper left), the Western US (upper right), Europe (lower left), and the Asia (lower right).

Currently, no passive microwave observations are used in operational analysis systems although the potential for SWE retrievals has been demonstrated (e.g. [20], [8], [16]). In this study, the SWE product derived from AMSR-E is used for comparisons with the operational global analyses from ECMWF. It has been demonstrated in previous studies that passive microwaves are insensitive to snow depths below 30 mm and above 750 mm [13]. Consequently, in the ECMWF analyses snow water equivalent below 10 mm and above 250 mm was set to 0 mm and 250 mm, respectively. In addition, the comparison shown in Figs. 5 and 6 are based on the AMSR-E data available. Strong fluctuations in mean SWE and extent are due to the AMSR-E overpasses with varying data coverage for a given area.

Mean daily snow extent is significantly lower in the AMSR-E data set when compared to the ECMWF analyses (Fig. 5). Especially for the first half of the snow season the differences between the AMSR-E data set and

the analyses are much larger than the differences between the two analyses. During the melting season the agreement between the three data sets is reasonable. Snow water equivalent derived from AMSR-E tends to be lower than the analyses in the US and Europe. Surprisingly, there is good agreement between the data sets is in the Western US. In this area, the AMSR-E product supports the OA. In Europe and Asia, the ROA yields systematically higher SWE values than the OA. Since the satellite data should mainly influence the snow edge, it is likely that these differences are introduced by omitting climatology in the ROA. However, this preliminary comparison suggests that the AMSR-E data set is not accurate enough to validate the analyses.
The comparisons described in this section are based on regions where the occurence of snow is possible according to the AMSR-E SWE algorithm described in section 2.1. Therefore, the values presented in Figs. 5 and 6 must not be compared directly with the data shown in Figs. 3 and 4.

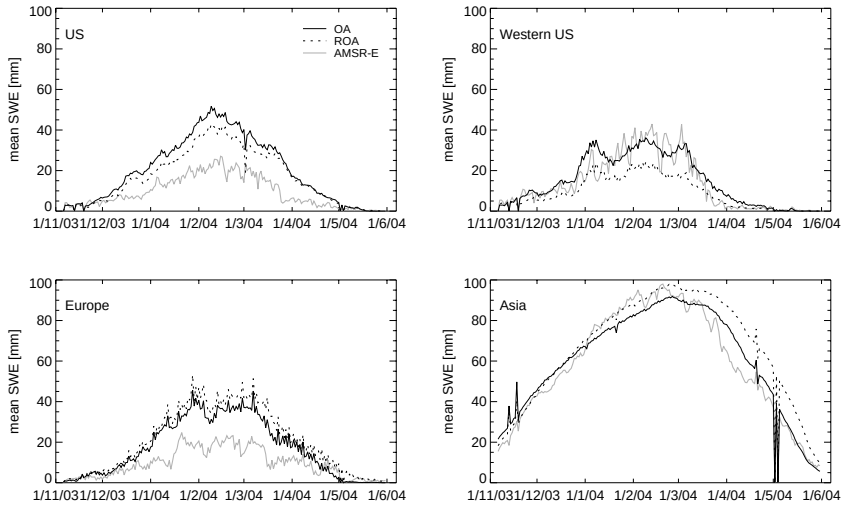

Figure 6: Mean daily snow water equivalent for the US (upper left), the Western US (upper right), Europe (lower left), and Asia (lower right).

3.3 Analysis increments

To analyse the differences in the ECMWF SWE products it is interesting to compare the analysis increments, i.e. the difference between analysis and the first guess. For the snow accumulation period from November 6 to January 31 mean analysis increments have been computed based on the sum of the 06 UTC and 12 UTC analyses (Fig. 7).
For the Eurasian land mass (East of 40° E) almost no in-situ observations are available at 06 UTC and 12 UTC. The analysis increments obtained through the ROA are basically introduced through the NOAA NESDIS satellite observations. It can clearly be seen that the satellite data tend to reduce SWE at the snow edge. Areas north of 60° N remain almost unaffected. The increments in the OA are introduced through the relaxation to climatology. It is interesting to note that these values are of the same order of magnitude as the increments introduced by the satellite data. In addition, a band along 50° N characterized by negative increments can be found in both analyses.
Over Europe, the analysis increments are positive in both analyses. Observations enter the analyses mainly at 06 UTC, the satellite data are introduced at 12 UTC in the ROA. The analysis increments are generally smaller in the ROA. This can be attributed to the fact that the analysis increments at 06 UTC have not been cycled in the OA. A more detailed look on the individual increments at 06 UTC and 12 UTC for the ROA reveals that the observations tend to produce positive increments, whereas the satellite data result in negative increments. However, the spatial structure of increments at the two analyses times strongly depends on the time of the season.

For the North American domain, in-situ data and satellite observations are used simultaneously in the 12 UTC analyses. In both analyses, negative increments can be found for large parts of the West, which may explain the low SWE values compared to the SNODAS data set. However, in the OA positive increments are obtained for the Western mountain range. In contrast, the ROA has negative increments in this area. As a consequence, the ROA has less snow than the OA in the West. At this point it is not clear whether the use of climatology in the OA results in positive increments or whether the satellite data reduce the increments in the ROA. A more detailed analysis on the temporal evolution of the increments is needed. For the Canadian domain, mainly positive increments can be found in the OA. In the ROA the Western part of Canada is characterized by negative increments. Again, it is difficult to attribute these changes either to the influence of the snow climatology or to the usage of the satellite data.

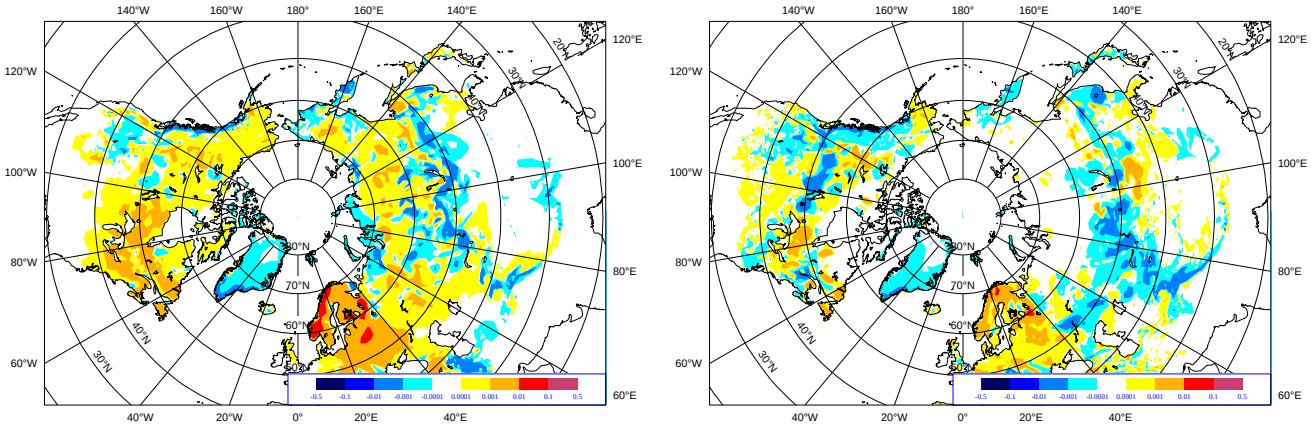

Figure 7: Mean analysis increments from 06 UTC and 12 UTC for the period from November 6 to January 31 for the OA (left image) and the ROA (right image).

4 Summary and conclusion

Combining modelled snow fields, in-situ measurements, and satellite observations in a data assimilation system is a challenging task. To the author's knowledge only two centres, namely the NOHRSC and ECMWF, merge the three data sources in their operational analyses. The NOHRSC product benefits from a high resolution model, a comparably dense observation network (including in-situ observations of snow water equivalent), and a data assimilation system that involves an analyst. Consequently, this SWE product should be regarded as the best operational data set available for the US. The ECMWF analysis is global and has to be fully automated.
In order to quantify the impact of satellite derived snow extent, two versions of the operational ECMWF analyses have been compared against the NOHRSC data set. It has been found that using satellite observations improves the analysed snow extent. This result is in agreement with earlier comparisons of analysed snow fields and MODIS derived snow extent ([11]). In general, the ECMWF analyses tend to underestimate snow water equivalent in the Western part of the United States. Negative analysis increments indicate that either the observations used in the analysis are not representative of the area means or that the climatology (in the OA) and the satellite data (in the ROA) remove too much SWE. Future work will have to focus on a more detailed comparison of additional data, e.g. snow fall, evaporation, and snow melt.
A direct comparison between the analysed SWE fields and AMSR-E derived SWE is difficult since the satellite observations are insensitive to low and high amounts of SWE. The differences between the two analyses and the satellite product are comparable to the differences between the analyses and the NOHRSC product. However, the results for the Western US indicate that AMSR-E derived SWE could be a useful source of information in the analysis system. Assimilating AMSR-E derived SWE in the Western US region could potentially result in

higher SWE values without changing the snow extent.
Spatial interpolation schemes (e.g. ECMWF's Cressman Interpolation) are appropriate to combine model snow fields and in-situ observations. To make optimal use of satellite data, future analysis systems have to be more sophisticated. Kalman Filtering as suggested by [2] could be one option. The development and improvement of forward operators, which link the modelled SWE to observed passive microwave brightness temperatures is one key issue. For the optimal usage of satellite derived snow extent, more realistic relationships between fractional snow extent and SWE have to be established and implemented in the numerical models.

Acknowledgements

The author would like to thank P. Viterbo, D. Vasiljevic, and E. Andersson (all ECMWF) for many helpful comments and J. Haseler (ECMWF) for her support with the technical implementation of the revised analysis scheme. The NOHRSC SNODAS and AMSR-E SWE data sets were obtained through NSIDC. R. Hine (ECMWF) helped with the preparation of the figures.

References

[1] E.A. Anderson. A point energy and mass balance model of snow cover. Technical Report NWS-19, US National Oceanic and Atmospheric Administration NOAA, Silver Spring, MD, US, 1976.

[2] K.M. Andreadis and D.P. Lettenmaier. Data assimilation of remotely sensed snow observations using an ensemble Kalman Filter. In A.J. Teuling, H. Leijnse, P.A. Troch, J. Sheffield, and E.F. Wood, editors, *Book of Abstracts - International Workshop on the terrestrial water cycle: Modelling and data assimilation across catchment scales*, page 168, Wageningen, The Netherlands, 2004. Wageningen University.

[3] R.L. Armstrong and M.J. Brodzig. Recent Northern Hemisphere snow extent: A comparison of data derived from visible and microwave satellite sensors. *Geophys. Res. Let.*, 28:3673–3676, 2001.

[4] A. Barrett. National Operational Hydrologic Remote sensing Center SNOw Data Assimilation System (SNODAS) Products at NSIDC. Special Report 11, NSIDC, Boulder, CO, US, 2003.

[5] T. Carroll, D. Cline, G. Fall, A. Nilsson, L. Li, and A. Rost. NOHRSC operations and the simulation of snow cover properties for the conterminous US. In *Proceedings of the 69th Annual Meeting of the Western Snow Conference*, pages 1–14, 2001.

[6] National Operational Hydrologic Remote Sensing Center. SNODAS Data Products at NSDIC. Technical report, NSIDC, Boulder, CO, 2004.

[7] A. Chang and A. Rango. AMSR-E/Aqua Daily L3 Global Snow Water Equivalent EASE-Grids V001. Technical report, NSIDC, Boulder, CO, 2004.

[8] A.T.C. Chang, J.L. Foster, D.K. Hall, B.E. Goodison, A.E. Walker, and J.R. Metcalfe. Snow parameters derived from microwave measurements during the BOREAS winter field experiment. *J. Geophys. Res.*, 102:29663–29672, 1997.

[9] R. Daley. *Atmospheric Data Analysis*. Cambridge University Press, Cambridge, UK, 1991.

[10] K.F. Dewey and R. Heim. Satellite observations of variations in northern hemisphere seasonal snow cover. Technical Report NESS 87, NOAA, 1981.

[11] M. Drusch, D. Vasilievic, and P. Viterbo. ECMWF's global snow analysis: Assessment and revision based on satellite observations. *J. Appl. Met.*, 43:1282–1294, 2004.

[12] D.J. Foster and R.D. Davy. Global snow depth climatology. Tech. Note TN-88/006, U.S. Air Force Environmental Technical Applications Center, 1988.

[13] J.L. Foster, A.T.C. Chang, R.J. Gurney, F. Hewer, and R. Essery. Snow cover and snow mass estimates from remote sensing, climatology and the United Kingdom Meteorological Office General Circulation Model. In B.J. Choudhury, Y.K. Kerr, E.G. Njoku, and P. Pampaloni, editors, *Passive Microwave Remote Sensing of Land-Atmosphere Interactions*, pages 55–76, Utrecht, The Netherlands, 1995. VSP.

[14] J. Haseler. Early-delivery suite. *ECMWF Newsletter*, 101:21–30, 2004.

[15] R. Jordan. User's guide for usa-crrel one dimensional snow temperature model (sntherm.89). Technical report, USA Cold Regions Research and Engineering Laboratory, 1990.

[16] R.E. Kelly, A.T.C. Chang, L. Tsang, and J.L. Foster. A prototype amsr-e global snow area and snow depth algorithm. *IEEE Trans. Geosc. Rem. Sens.*, 42:230–242, 2003.

[17] J.T. Pulliainen, J. Grandell, and Hallikainen M.T. Retrieval of surface temperature in boreal forest zone from SSM/I data. *IEEE Trans. Geosc. Rem. Sens.*, 35:1188–1200, 1997.

[18] D.A. Robinson, K.F. Dewey, and R.R. Heim. Global snow cover monitoring: An up-date. *Bull. Amer. Meteorol. Soc.*, 74:1689–1696, 1993.

[19] D.A. Robinson and G. Kukla. Maximum surface albedo of seasonally snow covered lands in the northern hemisphere. *J. Clim. Appl. Met.*, 24:402–411, 1985.

[20] C.Y. Sun, C.M.U. Neale, and J.J. McDonnell. Snow wetness estimates of vegetated terrain from satellite passive microwave data. *Hydrologic Proc.*, 10:1619–1628, 1996.